

# Acoustic Radiation From a Pulsating Spherical Cap Set on a Spherical Baffle Near a Hard/Soft Flat Surface

Seyyed M. Hasheminejad and Mahdi Azarpeyvand

**Abstract**—Radiation of sound from a spherical piston, set in the side of a rigid sphere, undergoing harmonic radial surface vibrations in an acoustic halfspace is analyzed in an exact fashion using the classical method of separation of variables. The method of images in combination with the translational addition theorems for spherical wave functions is employed to take the presence of the flat boundary into account. The analytical results are illustrated with numerical examples in which the piston is pulsating near the rigid/compliant boundary of a water-filled halfspace. Subsequently, the basic acoustic field quantities such as the acoustic radiation impedance load and the radiation intensity distribution are evaluated for representative values of the parameters characterizing the system. Numerical results reveal the important effects of excitation frequency, source position, and cap angle on the acoustic radiation impedance load and the radiation intensity distribution. The presented work can lead to a better understanding of dynamic response of near-surface underwater transducers.

**Index Terms**—Addition theorems, cap angle, radiation impedance, spherical piston.

## I. INTRODUCTION

**R**ADIATION and scattering problems which involve waves of one characteristic shape that are incident upon a boundary of some other shape are important problems with various practical applications in underwater acoustics, oceanic engineering and acoustics of surfaces and discontinuities. References [1] and [2] have each employed distinct analytical methods to examine acoustic scattering of plane compressional waves by two identical rigid and elastic spheres, respectively. The method of images in combination with the translational addition theorems for the spherical wave functions are extensively employed to study acoustic scattering by a hard spherical body near a hard flat boundary [3], by a thin spherical shell near a free (pressure release) surface [4], and by an ideal air-bubble near the sea surface [5]. Axisymmetric acoustic radiation from a spherical source vibrating with an arbitrary, time-harmonic velocity distribution while positioned wholly outside a fluid sphere is examined in [6]. Likewise, acoustic coupling between two finite-sized spherical sources in a boundless fluid medium is considered in [7] and [8]. In two more recent papers [9], [10], the latter analysis is generalized for a number of nonaxisymmetric spherical sources within a fluid sphere. Reference

[11] determines the modal impedances for axisymmetric oscillations of two neighboring spheres in a thermoviscous acoustic medium. The method of images is also employed in [12] to determine the modal impedances of a spherical source located close to a locally reacting (finite impedance) planar interface. Just recently, the energy distribution and modal impedances for general (nonaxisymmetric) radiation from a pair of arbitrarily positioned oscillating rigid spheres in an infinite fluid medium are examined [13].

The acoustic radiation impedance of pistons placed on baffles has extensively been considered in the literature for various piston and baffle geometries (i.e., planes, spheres, cylinders, and spheroids [14]–[20]). The self-radiation impedance for the classic problem of a radially (axially) vibrating piston set in a rigid sphere is presented in [14] and [15]. The mutual acoustic impedance of pistons on a sphere and a cylinder are analyzed in [16] and [17], respectively. Likewise, the acoustic radiation impedance of curved vibrating caps and rings located on hard baffles of prolate and oblate spheroidal obstacles are formulated in [18] and [19], respectively. Just lately, the self and mutual radiation impedances for rectangular piston sources vibrating on a rigid prolate spheroidal baffle have been investigated [20]. The present work studies acoustic radiation from a harmonically pulsating piston set in the side of a rigid spherical baffle that is located near a hard/soft planar interface. This configuration is a practical idealization for a baffled spherical transducer placed near a rigid/free surface.

## II. MATHEMATICAL FORMULATION

The problem can be analyzed by means of the standard methods of theoretical acoustics. The fluid is assumed to be inviscid and ideal compressible that cannot support shear stresses making the state of stress in the fluid purely hydrostatic. In view of the fact that the spherical cap is supposed to undergo time-harmonic surface pulsations, with frequency  $\omega$ , the field equations may conveniently be expressed in terms of a scalar velocity potential as [21]:

$$\mathbf{u} = -\nabla\Phi, \quad p = -i\omega\rho\Phi, \quad \nabla^2\Phi + k^2\Phi = 0 \quad (1)$$

where  $\rho$  is the ambient fluid density,  $\mathbf{u}$  is the fluid particle velocity vector,  $p$  is the acoustic pressure in the inviscid fluid,  $k = \omega/c$  is the acoustic wave number,  $c$  is the ideal speed of sound, and we have assumed harmonic time variations throughout with  $e^{-i\omega t}$  dependence suppressed for simplicity.

Manuscript received June 4, 2003; revised August 13, 2003.

The authors are with the Department of Mechanical Engineering, Iran University of Science and Technology, Narmak, Tehran 16844, Iran (e-mail: hashemi@iust.ac.ir).

Digital Object Identifier 10.1109/JOE.2003.822978

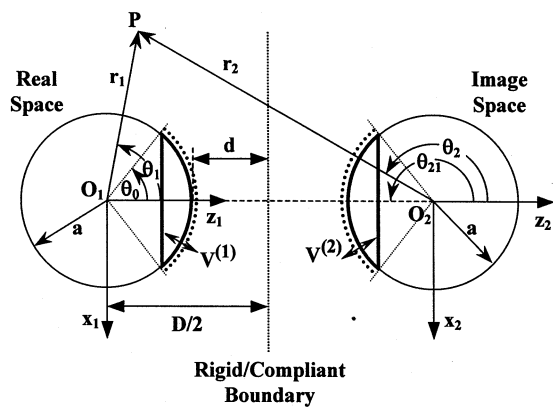


Fig. 1. The geometry of the spherical piston in the neighborhood of a flat reflecting boundary and its image.

Undoubtedly, the sound field radiated by a source may often be appreciably affected by a neighboring surface. In fact, the presence of a reflecting surface near a source can affect not only the directional properties of the source but also the total radiated sound power by the source [22]. Consider a spherical piston set on a rigid spherical baffle positioned at a finite distance from a flat wall (Fig. 1). It is clear that the proximity of the wall makes the problem more difficult to solve. If the wall is initially idealized as rigid, planar, and of infinite extent, a very simple theoretical device known as the method of images can smoothly take its presence into account [3]–[5], [21]. This method substitutes the original boundary value problem by one with two sources in an unbounded medium (i.e., the original source and the mirror image source). The mirror symmetry of the boundary value problem for two sources inherently leads to elimination of the normal component of the fluid velocity on the fictitious wall. Consequently, the solution to the problem with source-image configuration naturally satisfies the fluid-dynamic equations and the pertinent boundary conditions of the original problem.

The problem geometry is depicted in Fig. 1. The centers of the two spheres are separated by a distance  $D$  and the cap angle is  $\theta_0$ . The origins  $O_1$  and  $O_2$  of the two spherical coordinate systems  $(r_1, \theta_1, \varphi_1)$  and  $(r_2, \theta_2, \varphi_2)$  coincide with the centers of the real and imaginary spheres, respectively. The direct distance between center of the source and the receiver (field point) is  $r_1$ , the direct distance between center of the image source and the receiver (field point) is  $r_2$ . The dynamics of the present multi-scattering problem may be expressed in terms of two scalar potentials: one corresponding to the waves disseminating from the real sphere and the other relating to the waves from the image sphere. Each of these waves can be represented in form of an infinite (generalized Fourier) series whose unknown modal coefficients are to be determined by imposing the proper boundary conditions. Accordingly, for axisymmetric motion in bi-spherical coordinates we set

$$\begin{aligned}\Phi^{(1)}(r_1, \theta_1, \omega) &= \sum_{n=0}^{\infty} a_n(\omega) h_n(kr_1) P_n(\eta_1) \\ \Phi^{(2)}(r_2, \theta_2, \omega) &= \sum_{n=0}^{\infty} b_n(\omega) h_n(kr_2) P_n(\eta_2)\end{aligned}\quad (2)$$

where  $h_n() = j_n() + iy_n()$  is spherical Hankel function [24],  $n$  is the circumferential wave number,  $P_n(\eta_i)$  is Legendre function ( $\eta_i = \cos\theta_i$ ,  $i = 1, 2$ ), and  $a_n(\omega)$ ,  $b_n(\omega)$  are unknown modal coefficients.

The real sphere is supposed to be rigid except for a cap region ( $0 \leq \theta_1 \leq \theta_0$ ) that is vibrating radially with a prescribed velocity  $V^{(1)}$ . Similarly, the piston set in the surface of the image sphere is pulsating in the region  $\pi - \theta_0 \leq \theta_2 \leq \pi$  with a prescribed velocity  $V^{(2)}$ . The velocity of each piston can be expressed as a linear combination of spherical modes in the form of infinite series

$$\begin{aligned}v_1(\eta_1) &= \sum_{n=0}^{\infty} V_n^{(1)} P_n(\eta_1) = \begin{cases} V^{(1)} & 0 \leq \theta_1 \leq \theta_0 \\ 0 & \theta_0 \leq \theta_1 \leq \pi \end{cases} \\ v_2(\eta_2) &= \sum_{n=0}^{\infty} V_n^{(2)} P_n(\eta_2) = \begin{cases} 0 & 0 \leq \theta_2 \leq \pi - \theta_0 \\ V^{(2)} & \pi - \theta_0 \leq \theta_2 \leq \pi \end{cases}\end{aligned}\quad (3)$$

where  $V_n^{(1)}$  and  $V_n^{(2)}$  are the modal coefficients of surface velocity distributions. These coefficients can readily be determined after multiplying both sides of (3) by  $P_m(\eta)$ , ( $m = 0, 1, 2, \dots$ ), integrating over  $d\eta$ , and subsequently applying the orthogonality property of the Legendre functions:

$$\begin{aligned}V_n^{(1)} &= \left(n + \frac{1}{2}\right) V^{(1)} \int_{\eta_0}^1 P_n(\eta) d\eta \\ &= \frac{1}{2} [P_{n-1}(\eta_0) - P_{n+1}(\eta_0)] V^{(1)} \\ V_n^{(2)} &= \left(n + \frac{1}{2}\right) V^{(2)} \int_{-1}^{-\eta_0} P_n(\eta) d\eta \\ &= \frac{(-1)^n}{2} [P_{n-1}(\eta_0) - P_{n+1}(\eta_0)] V^{(2)}\end{aligned}\quad (4)$$

where the integrations are performed by using the following well-known relation [14]

$$(2n+1) \int_{\eta_0}^1 P_n(\eta) d\eta = P_{n-1}(\eta_0) - P_{n+1}(\eta_0)\quad (5)$$

Many radiation and scattering problems involve waves of one characteristic shape (coordinate system) that are incident upon a boundary of some other shape (coordinate system). So it is difficult to satisfy the boundary conditions on that surface. There exists, however, a class of mathematical relationships called wave transformations that circumvent this difficulty in many cases by allowing one to express the incident wave in terms of wave functions for some other coordinate system which is more appropriate to the boundary, i.e., they simply permit the study of the fields scattered by the various bodies, all referred to a common origin [9]. This transformation (shift of origin) of the wave functions greatly simplifies the task of satisfying the specified boundary conditions on the various surfaces. In particular, to fulfil orthogonality in the current problem (Fig. 1), we need to express the spherical wave functions of the  $(r_1, \theta_1)$  coordinate system in terms of spherical wave functions of the  $(r_2, \theta_2)$  coordinate system, and vice versa, through application of the

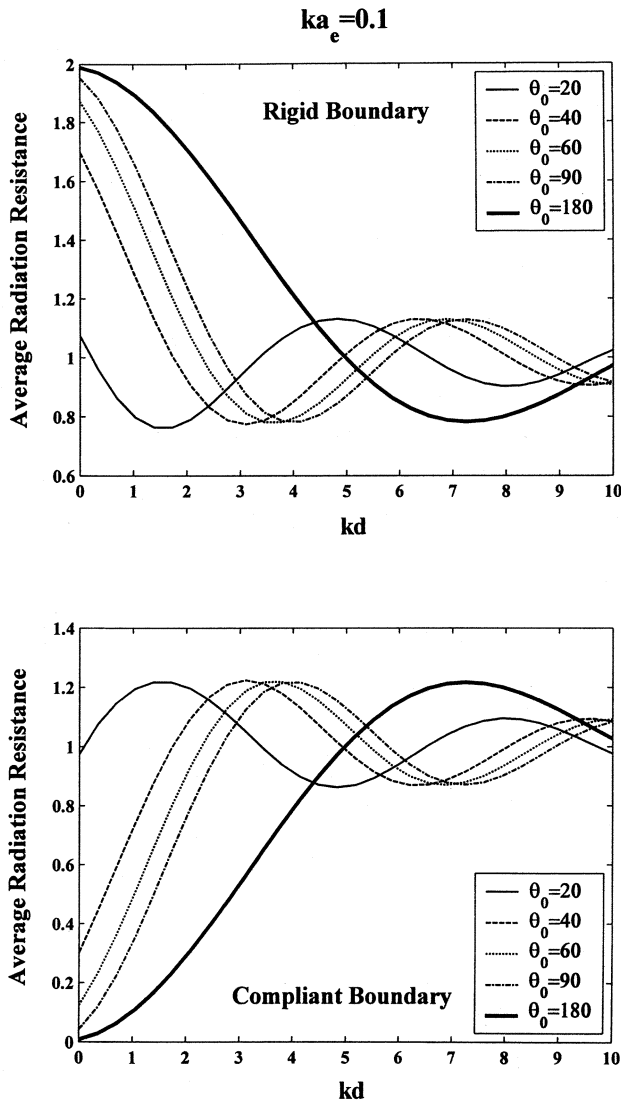


Fig. 2. Normalized resistance component of a spherical piston, pulsating at the excitation frequency of  $ka_e = 0.1$  near a rigid/compliant interface, versus  $kd$  for various cap angles.

classical form of translational addition theorem for bi-spherical coordinates [23]:

$$h_n(kr_s)P_n(\cos\theta_s) = \begin{cases} \sum_{m=0}^{\infty} Q_{mn}(kr_{sl}, \theta_{sl}) j_m(kr_l) P_m(\cos\theta_l), & r_l < r_{sl} \\ \sum_{m=0}^{\infty} R_{mn}(kr_{sl}, \theta_{sl}) h_m(kr_l) P_m(\cos\theta_l), & r_l > r_{sl} \end{cases} \quad (6)$$

where  $s, l = 1, 2 (s \neq l)$ ,  $j_n(\cdot)$  is spherical Bessel function of order  $n$  [24],  $\theta_{sl}$  is the angle between the  $z_s$  axis and the  $O_s O_l$  line (i.e., such that  $\theta_{12} = 0$  or  $\theta_{21} = \pi$ ),  $r_{12} = r_{21} = D$  is the center to center distance (Fig. 1), and

$$Q_{mn}(kr_{sl}, \theta_{sl}) = i^{m-n} (2m+1) \sum_{\sigma=|m-n|}^{m+n} i^{\sigma} b_{\sigma}^{nm} \times h_{\sigma}(kr_{sl}) P_{\sigma}(\cos\theta_{sl})$$

$$R_{mn}(kr_{sl}, \theta_{sl}) = i^{m-n} \sum_{\sigma=|m-n|}^{m+n} i^{\sigma} (2\sigma+1) \times b_{\sigma}^{nm} j_{\sigma}(kr_{sl}) P_{\sigma}(\cos\theta_{sl}) \quad (7)$$

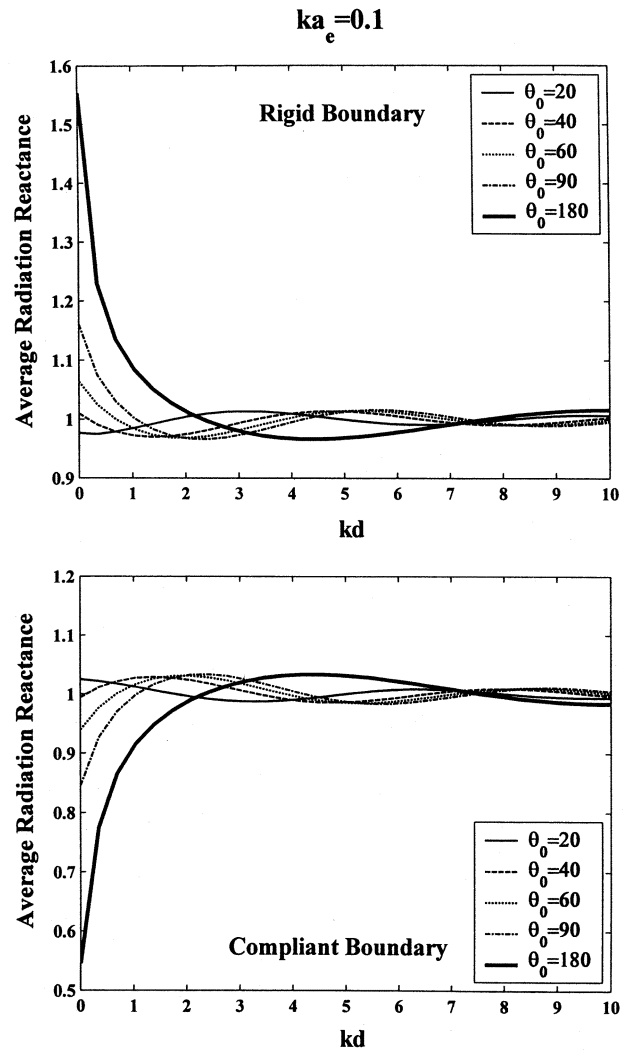


Fig. 3. Normalized reactance component of a spherical piston, pulsating at the excitation frequency of  $ka_e = 0.1$  near a rigid/compliant interface, versus  $kd$  for various cap angles.

where  $b_{\mu}^{nm} = (nm00|\mu0)^2$ , in which Clebsch-Gordan Coefficients are defined, with  $q = (\mu + n + m)/2$  and  $2q$  being even, as [23]

$$(nm00|\mu0) = \frac{(-1)^{\mu+q} q!}{(q-n)!(q-m)!(q-\mu)!} \times \sqrt{\frac{(2\mu+1)!}{(2q+1)!} (2q-2n)!(2q-2m)!(2q-2\mu)!} \quad (8)$$

and when  $2q$  is odd,  $(mm00|\mu0) = 0$ .

Incorporation of the above addition theorem in (2) allows us to translate the wave components of the first coordinate system in terms of spherical wave functions of the second coordinate system, and vice versa, i.e.,

$$\Phi^{(1)}(r_2, \theta_2, \omega) = \sum_{n=0}^{\infty} \sum_{m=0}^{\infty} Q_{mn}(kD, 0) a_m(\omega) \times j_n(kr_2) P_n(\eta_2)$$

$$\Phi^{(2)}(r_1, \theta_1, \omega) = \sum_{n=0}^{\infty} \sum_{m=0}^{\infty} Q_{mn}(kD, \pi) b_m(\omega) \times j_n(kr_1) P_n(\eta_1) \quad (9)$$

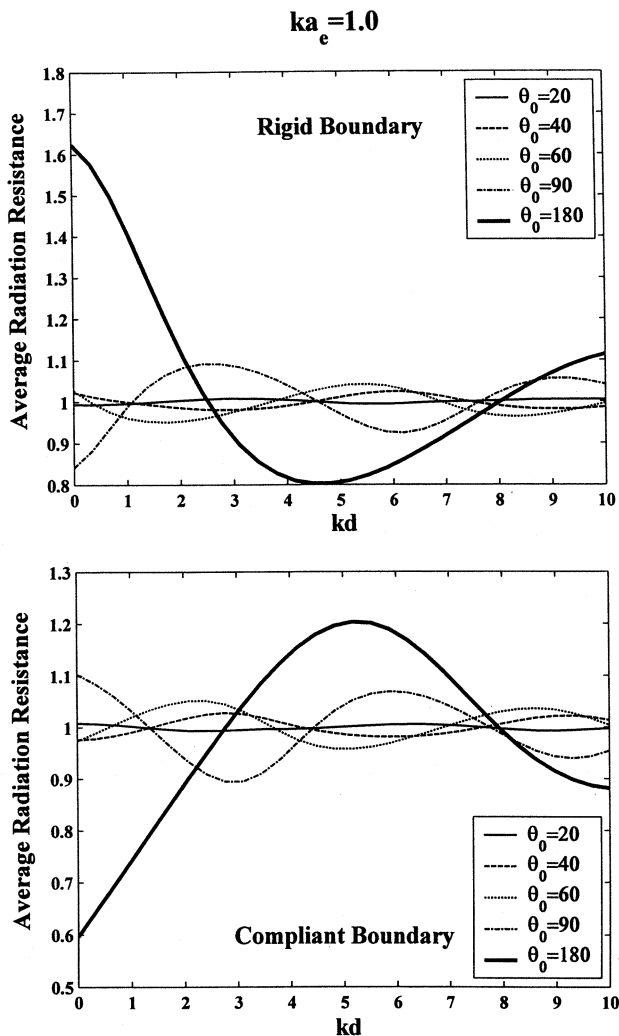


Fig. 4. Normalized resistance component of a spherical piston, pulsating at the excitation frequency of  $ka_e = 1$  near a rigid/compliant interface, versus  $kd$  for various cap angles.

The modal coefficients,  $a_m(\omega)$  and  $b_m(\omega)$  must be determined by imposing the suitable boundary conditions. The continuity of radial velocity components at the surface of each sphere implies that

$$-\left. \frac{\partial \Phi(r_i, \theta_i, \omega)}{\partial r_i} \right]_{r_i=a} = \sum_{n=0}^{\infty} V_n^{(i)} P_n(\eta_i) \quad (10)$$

where  $\Phi(r_i, \theta_i, \omega) = \Phi^{(1)}(r_i, \theta_i, \omega) + \Phi^{(2)}(r_i, \theta_i, \omega)$ , ( $i = 1, 2$ ). Substitution of the velocity potential expansions (2) and (9) into the above boundary conditions leads to

$$\begin{aligned} & \left( n + \frac{1}{2} \right) [P_{n+1}(\eta_0) - P_{n-1}(\eta_0)] V^{(1)} \\ & = kh'_n(ka) a_n(\omega) + kj'_n(ka) \sum_{m=0}^{\infty} Q_{mn}(kD, \pi) b_m(\omega) \\ & (-1)^n \left( n + \frac{1}{2} \right) [P_{n+1}(\eta_0) - P_{n-1}(\eta_0)] V^{(2)} \\ & = kj'_n(ka) \sum_{m=0}^{\infty} Q_{mn}(kD, 0) a_m(\omega) + kh'_n(ka) b_n(\omega) \quad (11) \end{aligned}$$

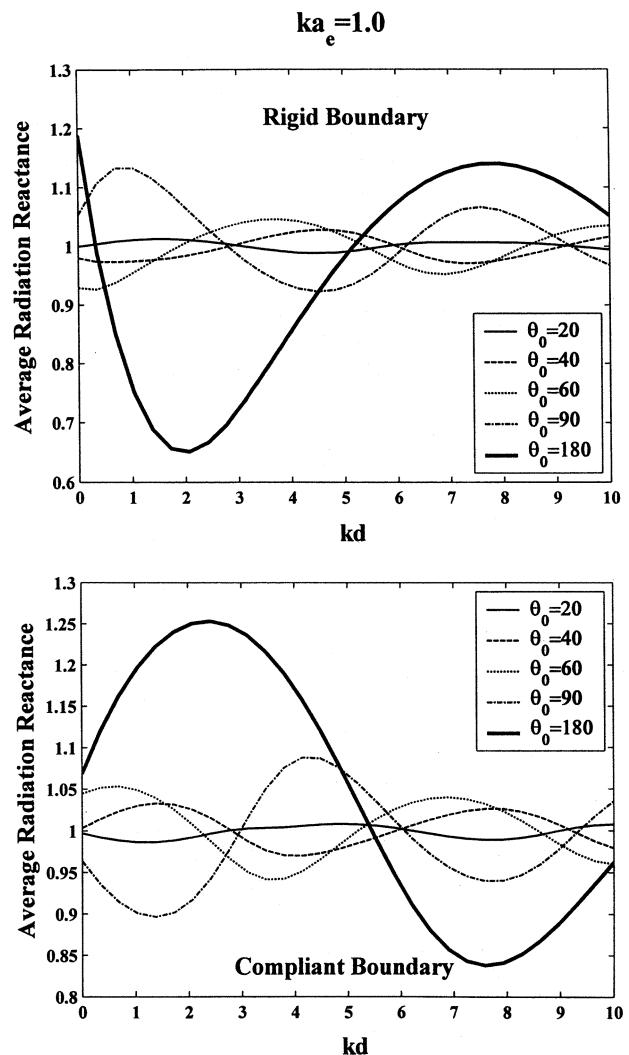


Fig. 5. Normalized reactance component of a spherical piston, pulsating at the excitation frequency of  $ka_e = 1$  near a rigid/compliant interface, versus  $kd$  for various cap angles.

where the prime symbol indicates the derivative with respect to the argument.

The fluctuating fluid pressure on the surface of a vibrating source constitutes its radiation loading. The normalized average acoustic radiation impedance load per unit area on the vibrating piston may be computed by making use of Foldy's definition based on the radiated power [15], [25]

$$\begin{aligned} Z_p(\omega) &= R_p(\omega) - iX_p(\omega) \\ &= \frac{1}{4\pi\rho c (V^{(1)}a_e)^2} \int_{\eta_0}^1 p(r_1=a, \eta_1, \omega) v_1^*(\eta_1) d\eta_1 \quad (12) \end{aligned}$$

where  $a_e = a \sin(\theta_0/2)$  is the effective piston radius (i.e., the radius of the sphere that has the same area as the piston),  $\rho c$  is characteristic impedance, the asterisk indicates complex conjugate, and  $R_p(\omega)$  and  $X_p(\omega)$  are the average acoustic resistance and reactance, respectively. Moreover  $p(a, \theta_1, \omega)$  is the acoustic

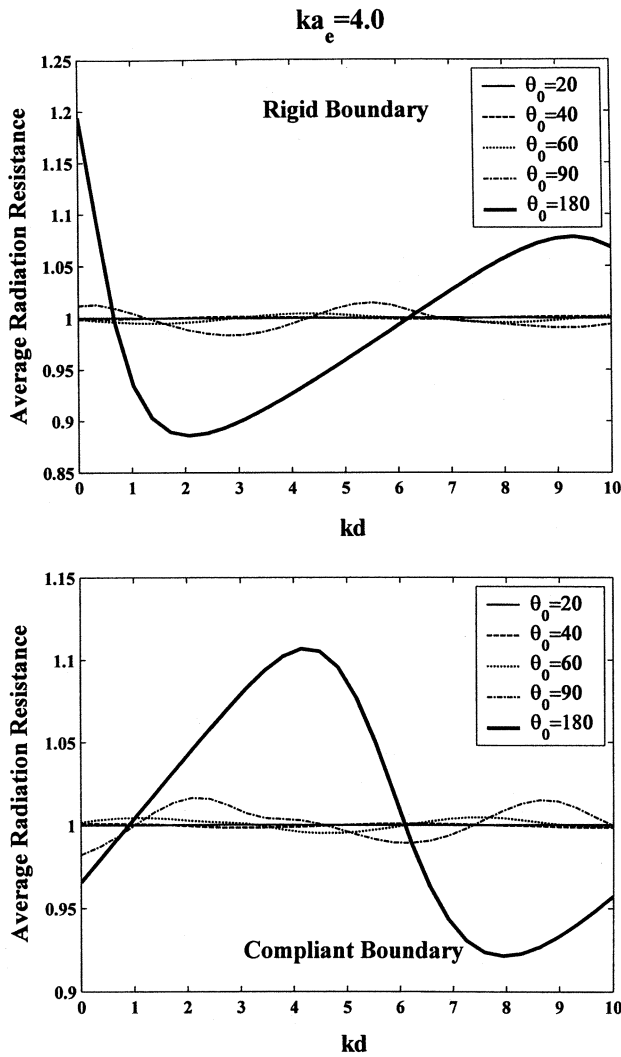


Fig. 6. Normalized resistance component of a spherical piston, pulsating at the excitation frequency of  $ka_e = 4$  near a rigid/compliant interface, versus  $kd$  for various cap angles.

pressure on the surface of the real sphere which can be readily obtained, by incorporating (2) and (9) in second of (1), as

$$\begin{aligned} p(r_1, \theta_1, \omega) \Big|_{r_1=a} &= -i\omega\rho\Phi(r_1, \theta_1, \omega) \Big|_{r_1=a} \\ &= -i\omega\rho \sum_{n=0}^{\infty} \Gamma_n(a, \omega) P_n(\eta_1) \end{aligned} \quad (13)$$

where

$$\Gamma_n(a, \omega) = h_n(ka) a_n(\omega) + j_n(ka) \sum_{m=0}^{\infty} Q_{mn}(kD, \pi) b_m(\omega) \quad (14)$$

Incorporating (13) in (12), after performing the integration, we obtain

$$Z_p(\omega) = \frac{k}{4\pi a_e^2 V^{(1)}} \sum_{n=0}^{\infty} \frac{P_{n-1}(\cos\theta_0) - P_{n+1}(\cos\theta_0)}{2n+1} \Gamma_n(a, \omega) \quad (15)$$

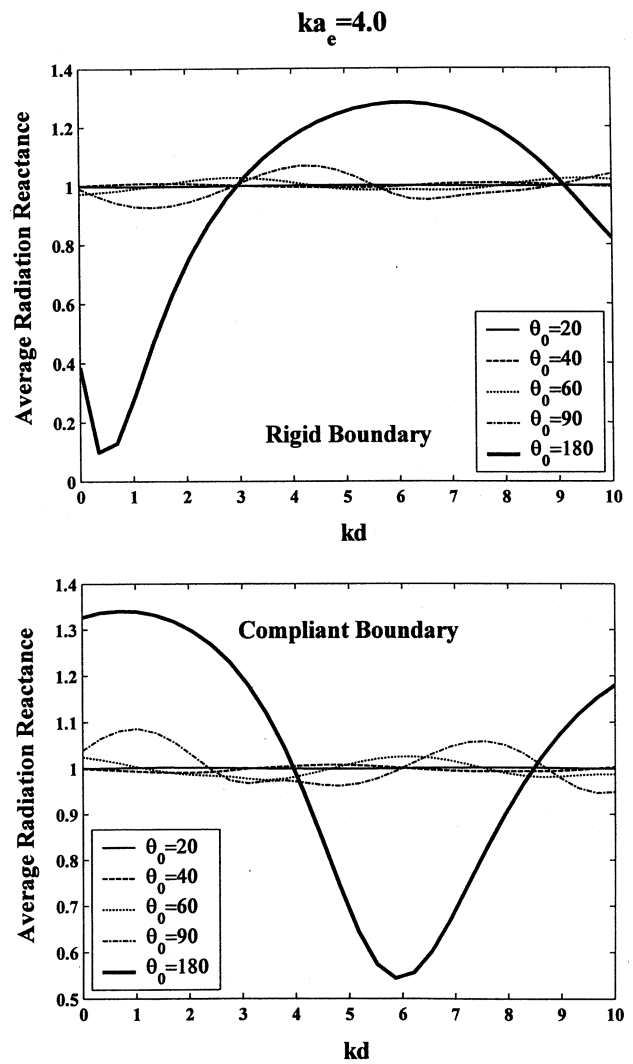


Fig. 7. Normalized reactance component of a spherical piston, pulsating at the excitation frequency of  $ka_e = 4$  near a rigid/compliant interface, versus  $kd$  for various cap angles.

In addition, the radial component of the acoustic power flux vector (acoustic intensity) radiated per unit solid angle from the real sphere is found from [21]

$$I_{rad} = \frac{1}{2} Re \left\{ p(r_1, \theta_1, \omega) \times \left[ \frac{-\partial\Phi(r_1, \theta_1, \omega)}{\partial r_1} \right]^* \right\} \quad (16)$$

### III. NUMERICAL RESULTS AND DISCUSSION

In order to illustrate the nature and general behavior of the solution, we consider a numerical example in this section. Realizing the crowd of parameters and the intense computations involved here, no attempt is made to exhaustively evaluate the effect of varying each of them. Accordingly, we confine our attention to a particular model. The surrounding ambient fluid is assumed to be water at atmospheric pressure and 300 kelvin ( $\rho = 0.997 \text{ g/cm}^3$ ,  $c = 149700 \text{ cm/s}$ ). The piston, which is set on a rigid spherical baffle of radius  $a = 1 \text{ cm}$ , is assumed to be

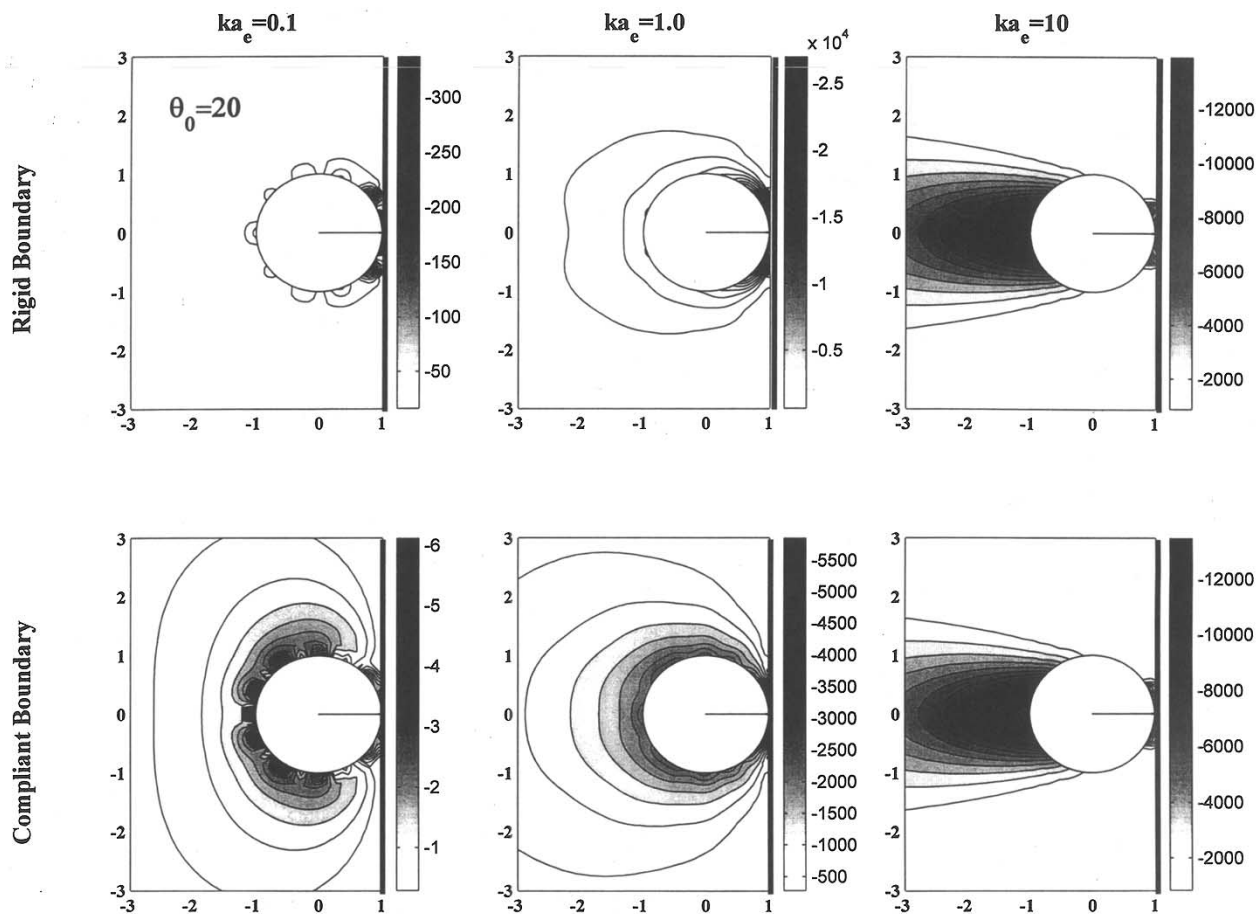


Fig. 8. Radiation intensity distribution in the vicinity of the spherical piston ( $\theta_0 = 20^\circ$ ) touching the halfspace boundary.

pulsating at the nondimensional frequencies of  $ka_e = \omega a_e / c = 0.1, 1, 4$  with selected cap angles of  $\theta_0 = 20^\circ, 40^\circ, 60^\circ, 90^\circ$  and  $180^\circ$ . A MATLAB code was constructed for treating boundary conditions, to determine the unknown modal coefficients, and to compute the average acoustic radiation impedance, and the acoustic radiation intensity as functions of the distance parameter  $kd$  and the cap angle  $\theta_0$  at selected nondimensional frequencies. Accurate computations for derivatives of spherical Bessel functions were accomplished by utilizing (10.1.19) and (10.1.22) in [24]. The computations were performed on a Pentium IV personal computer with a truncation constant of  $N = 35$  to assure convergence in the high frequency range, and also in case of close proximity of the source to the halfspace boundary.

Fig. 2 through 7 display the effects of distance parameter  $kd$  and the cap angle  $\theta_0$  on the inertial and the resistive components of the average acoustic radiation impedance at selected nondimensional frequencies ( $ka_e = 0.1, 1, 4$ ). In these figures, all of the resistance and reactance components are normalized with respect to the corresponding value of a single radiator in a boundless medium (i.e. to the value when the source is infinitely far removed from the halfspace boundary). Furthermore, in order to take the presence of the rigid (compliant) boundary into account by using the method of images, we have assumed in-phase (anti-phase) pulsations for both radiators, i.e.,  $V^{(1)} = V^{(2)}$  ( $V^{(1)} = -V^{(2)}$ ) [12], [13]. Comparison of the figures leads to following important observations. At the lowest

excitation frequency ( $ka_e = 0.1$ ), when the radiator is pulsating very close to the rigid (compliant) boundary, the normalized resistance magnitude approaches the value of two (zero) as the cap angle is increased to  $\theta_0 = 180$  (i.e., for a wholly pulsating sphere [7]). Furthermore, increasing the cap angle in the rigid (compliant) boundary case leads to a drastic increase (decrease) in the resistance magnitudes. This interesting result indicates that a small piston pulsating at low frequencies ( $ka_e \ll 1$ ) near a compliant (rigid) surface can be a far more (less) efficient radiator than a wholly pulsating sphere. Also, increasing the cap angle at this frequency causes a noticeable increase (decrease) in the reactance or added mass values when the source is positioned very close to the rigid (compliant) boundary (i.e., for  $kd \rightarrow 0$ ). As the separation parameter  $kd$  is increased, all the curves oscillate about and approach the free field value of unity. Moreover, as the nondimensional frequency is raised (i.e.,  $ka_e = 1, 4$ ), we observe relatively low (high) amplitude impedance curve oscillations for small (large) cap angles at all separation parameters. Thus, one can conclude that at relatively high frequencies, the presence of the rigid/compliant interface has a critical effect on the impedance components only for very large cap angles (i.e.,  $\theta_0 > 90^\circ$ ).

To further assess the effect of halfspace boundary on the acoustic field, the radiation intensity distribution at selected nondimensional frequencies of  $ka_e = 0.1, 1, 10$  in the neighborhood of a spherical piston that is almost touching

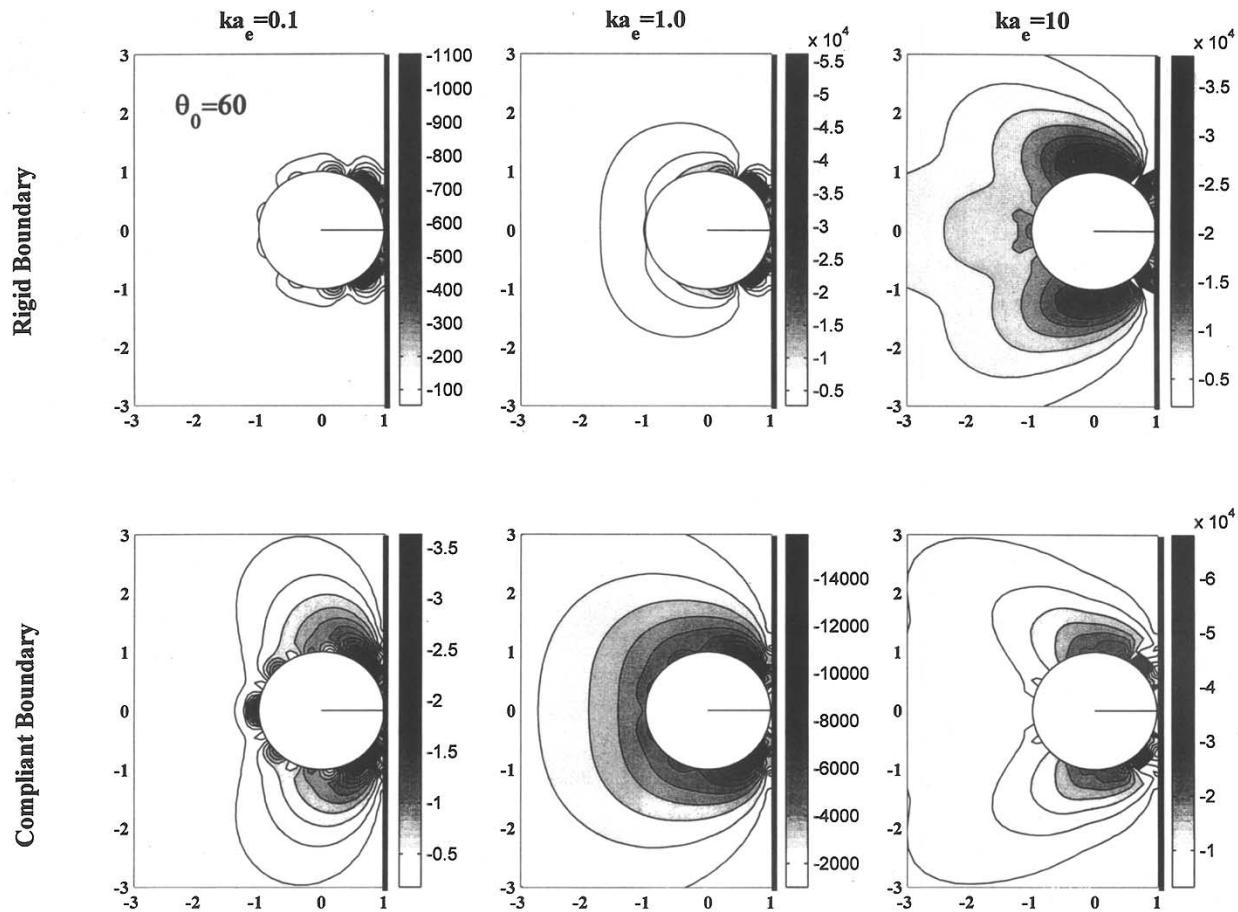


Fig. 9. Radiation intensity distribution in the vicinity of the spherical piston ( $\theta_0 = 60^\circ$ ) touching the halfspace boundary.

the rigid/compliant boundary for cap angles of  $\theta_0 = 20^\circ$  and  $60^\circ$  are presented in Figs. 8 and 9, respectively. It is very interesting to study the change in strength and directionality of the radiated energy as the excitation frequency, cap angle, and the halfspace boundary-type are changed. First, in all cases we notice a strong sound energy concentration in the gap area near the surface of piston, especially in the  $\theta_0 = 60^\circ$  case. As the excitation frequency is increased, sound energy concentration areas begin to expand and shift more uniformly around the spherical radiator. Next, increasing the cap angle leads to a general increase in the sound intensity amplitude. Furthermore, the intensity contours corresponding to the rigid wall case normally display higher levels, especially at the low and intermediate frequencies (i.e.,  $ka_e = 0.1, 1$ ). In addition, at the highest nondimensional frequency ( $ka_e = 10$ ), we note a quite strong backward radiation (i.e., away from the flat interface) in the  $\theta_0 = 20^\circ$  case, while a fairly strong forward (side-ward) radiation pattern is observed in the  $\theta_0 = 60^\circ$  situation.

Finally, to check overall validity of the work, we primarily note that the impedance component curves corresponding to the wholly pulsating sphere ( $\theta_0 = 180^\circ$ ) in Figs. 2 through 7 accurately duplicate the numerical results presented in [7]. Further numerical verifications are made by executing our general code for the case of a spherical cap positioned very far ( $d = 100a$ ) from the planar interface. Fig. 10 shows that the corresponding

radiation impedance components precisely reduce to the curves appearing in Fig. 20.4, page 308 in [14].

#### IV. CONCLUSION

Acoustic radiation impedance curves have been generated for a baffled pulsating spherical piston immersed near the rigid/compliant boundary of an acoustic halfspace. These curves are product of an exact multi-scattering treatment that involves utilization of the translational addition theorem for spherical wave functions in combination with the classical method of images. Numerical results reveal the important effects of excitation frequency, source position, and cap angle on the average acoustic radiation impedance load and the radiation intensity distribution. They demonstrate that a small piston pulsating at low nondimensional frequencies ( $ka_e \ll 1$ ) near a compliant (rigid) surface is a far more (less) efficient radiator than a wholly pulsating sphere. Furthermore, at relatively high nondimensional frequencies, the presence of the flat interface has a critical effect on the impedance values only for very large cap angles ( $\theta_0 > 90^\circ$ ). The presented work, which is an idealized model for acoustic radiation from a near-interface baffled spherical transducer, can be of interest in underwater acoustics and ocean engineering.

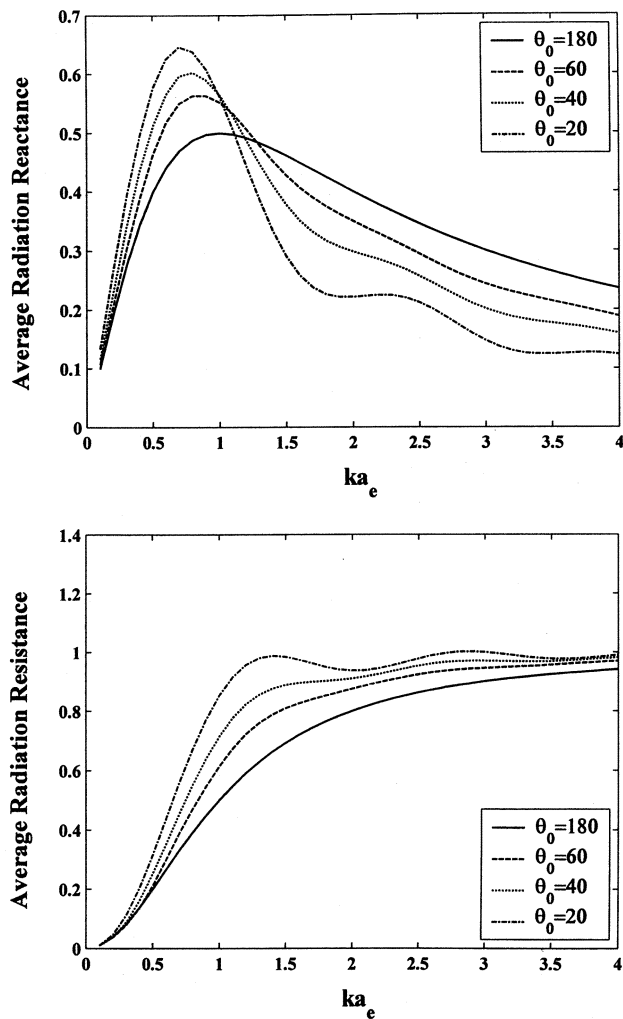


Fig. 10. Acoustic radiation impedance components for a baffled pulsating spherical cap, positioned very far from the planar interface ( $d = 100a$ ), as a function of  $ka_e$ .

#### REFERENCES

- [1] G. C. Gaunard, H. Huang, and H. C. Strifors, "Acoustic scattering by a pair of spheres," *J. Acoust. Soc. Amer.*, vol. 98, pp. 495–507, 1995.
- [2] P. Gabrielli and M. Mercier-Finidori, "Acoustic scattering by two spheres: multiple scattering and symmetry considerations," *J. Sound Vib.*, vol. 241, pp. 423–439, 2001.
- [3] G. C. Gaunard and H. Huang, "Sound scattering by a spherical object near a hard flat bottom," *IEEE Trans. Ultrason., Ferroelect., Freq. Contr.*, vol. 43, pp. 690–700, 1996.
- [4] H. Huang and G. C. Gaunard, "Scattering of a plane acoustic wave by a spherical elastic shell near a free surface," *Int. J. Solids Structures*, vol. 34, pp. 591–602, 1997.
- [5] G. C. Gaunard and H. Huang, "Acoustic scattering by an air-bubble near the sea surface," *IEEE J. Oceanic Eng.*, vol. 20, no. 4, pp. 285–292, 1995.
- [6] W. Thompson Jr., "Radiation from a spherical acoustic radiator near a scattering sphere," *J. Acoust. Soc. Amer.*, vol. 60, pp. 781–787, 1976.
- [7] —, "Acoustic coupling between two finite-sized spherical radiators," *J. Acoust. Soc. Amer.*, vol. 62, pp. 8–11, 1977.
- [8] —, "Acoustic coupling between a pulsating and an oscillating sphere," *J. Acoust. Soc. Amer.*, vol. 74, pp. 1050–1148, 1983.
- [9] S. A. Lease and W. Thompson Jr., "Use of translational addition theorems for spherical wave functions in a nonaxisymmetric acoustic field problems," *J. Acoust. Soc. Amer.*, vol. 90, pp. 1155–1160, 1991.
- [10] —, "Nonaxisymmetric acoustic radiation from a pair of radiators embedded in a fluid sphere," *J. Acoust. Soc. Amer.*, vol. 90, pp. 1161–1166, 1991.

- [11] M. Hasheminejad and T. L. Geers, "Modal impedance for two spheres in a thermoviscous fluid," *J. Acoust. Soc. Amer.*, vol. 94, pp. 2205–2214, 1993.
- [12] S. M. Hasheminejad, "Modal acoustic on a spherical radiator in an acoustic halfspace with locally reacting boundary," *acta-acustica-ACUSTICA*, vol. 87, pp. 443–453, 2001.
- [13] S. M. Hasheminejad and M. Azarpeyvand, "Non-axisymmetric acoustic radiation from a transversely oscillating rigid sphere above a rigid/compliant planar boundary," *Acta Acustica*, vol. 89, pp. 998–1007, 2003.
- [14] E. Skudrzyk, *The Foundations of Acoustics*. New York: Springer-Verlag, 1971.
- [15] P. M. Morse, *Vibration and Sound*: Acoust. Soc. Amer., Amer. Inst. Phys., 1981.
- [16] C. H. Sherman, "Mutual radiation impedance of sources on a sphere," *J. Acoust. Soc. Amer.*, vol. 31, pp. 947–952, 1959.
- [17] J. E. Greenspon and C. H. Sherman, "Mutual-radiation impedance and near field pressure for pistons on a cylinder," *J. Acoust. Soc. Amer.*, vol. 36, pp. 149–153, 1964.
- [18] A. L. Van Buren, "Acoustic radiation impedance of caps and rings on prolate spheroids," *J. Acoust. Soc. Amer.*, vol. 50, pp. 1343–1356, 1971.
- [19] R. Baier, "Acoustic radiation impedance of caps and rings on oblate spheroidal baffles," *J. Acoust. Soc. Amer.*, vol. 51, pp. 1705–1716, 1972.
- [20] J. E. Boisvert and A. L. Van Buren, "Acoustic radiation impedance of rectangular pistons on prolate spheroids," *J. Acoust. Soc. Amer.*, vol. 111, pp. 867–874, 2002.
- [21] A. D. Pierce, *Acoustics; an Introduction to Its Physical Principles and Applications*. New York: Amer. Inst. Phys., 1991.
- [22] D. A. Bies, "Effect of a reflecting plane on an arbitrary multipole," *J. Acoust. Soc. Amer.*, vol. 33, pp. 286–288, 1961.
- [23] Y. A. Ivanov, *Diffraction of Electromagnetic Waves on Two Bodies*, Minsk: Nauka i Tekhnika, 1968; NASA Tech. Transl. F-597, 1970.
- [24] M. Abramowitz and I. A. Stegun, *Handbook of Mathematical Functions*. Washington, DC: National Bureau of Standards, 1965.
- [25] W. Thompson Jr., "Acoustic radiation from a spherical source embedded eccentrically within a fluid sphere," *J. Acoust. Soc. Amer.*, vol. 54, pp. 1694–1707, 1973.



**Seyyed M. Hasheminejad** was born in Tehran, Iran, on July 6, 1962. He received the B.S. degree in mechanical engineering, in 1983, from California State University, Chico; M.S. degree in mechanical engineering, in 1985, from Santa Clara University, California; and Ph.D. degree in mechanical engineering, in 1992, from University of Colorado, Boulder.

Since 1993, he has been an assistant professor at the mechanical engineering department of Iran University of Science and Technology, Tehran. He has also been a part-time lecturer at Research Division of Azad University, Tehran, since 1999. He has conducted (consulted in) various national research projects, including design and construction of high-power underwater piezoelectric transducers, automotive acoustic silencers, sound absorbers (acoustic foams) and insulators, vibration damping treatments, pneumatic mounts, broadcasting studios; and noise and vibration control in automobiles, airplanes, trains, residential and industrial environments. He is currently involved in development of national standards, specifications and guidelines on environmental noise and vibration control.

Dr. Hasheminejad is a member of various professional societies in Iran such as the Iranian Society of Mechanical Engineers, Iranian Society of Electrical Engineers, and Iranian Society of Aerospace Engineers. He is an active reviewer for various journals and evaluating boards, and a member of several technical committees in professional societies in Iran.



**Mahdi Azarpeyvand** was born in Tehran, Iran, in 1981. He was among the top student entries through the National Iranian Higher Education Exam. Since 1999, he is working at Iran University of Science and Technology toward the B.S. degree in mechanical engineering. His research interests include scattering, wave propagation, and boundary value problems in electromagnetics and acoustics. He is a member of various student societies such as the student branch of Iranian Society of Mechanical Engineers and Iranian Physics Society. He has received several awards

as an outstanding student researcher.